

Highly sensitive temperature and strain sensors based on all-fiber 45°-TFG Lyot filter

Zhijun Yan *, Adebayo Adedotun, Kaiming Zhou, Lin Zhang
Photonics Research Group, Aston University, Birmingham, UK, B4 7ET
Corresponding author: yanz1@aston.ac.uk

ABSTRACT

We demonstrate highly sensitive temperature and strain sensors based on an all-fiber Lyot filter structure, which is formed by concatenating two 45°-TFGs (tilted fiber gratings) with a PM fiber cavity. The experiment results show the all-fiber 45°-TFG Lyot filter has very high sensitivity to strain and temperature. The 45°-TFG Lyot filters of two different cavity lengths (18cm and 40 cm) have been evaluated for temperature sensing by heating a section of the cavity from 10°C to 50°C. The experiment results have shown remarkably high temperature sensitivities of 0.616nm/°C for 18cm and 0.31nm/°C for 40cm long cavity filter, respectively. The 18cm long cavity filter has been subjected to strain variations up to around 550 $\mu\epsilon$ and the filter has exhibited strain sensitivities of 0.02499nm/ $\mu\epsilon$ and 0.012nm/ $\mu\epsilon$ for two straining situations, where its cavity middle section of 18cm and 9cm were stretched, respectively. .

Keywords: temperature, strain, sensor, Lyot filter, TFG

1. INTRODUCTION

Due to immunity of electro-magnetic field, compactness, physical flexibility, ease of fabrication, and the possibility of use in harsh environments, optical fiber based sensors have been widely used to monitor the structure condition and environmental parameters in industrial applications. The physic measurements by fiber-optic sensors include displacement, vibration, strain, temperature, humidity, pressure and so on [1-3]. Over the last twenty years, temperature and strain sensors based on fiber Bragg gratings (FBGs) have attracted more interests in civil engineering, power station, and aerospace [4-6]. However, such grating based sensors have relative low sensitivity, especially low for high resolution measurements. The typical temperature and strain sensitivities of standard FBGs around 1550nm are only 10pm/°C and 1pm/ $\mu\epsilon$ [7]. Recently, some researchers have reported sensors based on all fiber interferometer [8-10]. By monitoring the shift of transmission spectra of the interferometer, the changing of environmental parameters were detected, as the cavity is influenced by the environmental condition. In general, interferometer based sensors are more sensitive than FBG based ones and are suitable for small range high resolution sensing.

The Lyot filter is a polarization dependence interferometer [11], which is consisting of two linear polarizers and a birefringent crystal with its polarization axis aligned at 45° with respect to the fast (or slow) axes of the polarizers. Lyot filters have been applied in spectral imaging, communication, and laser systems [12-14]. The traditional Lyot

filter was constructed by two bulk linear polarizers and one birefringence crystal [12], which was not convenient for integration. Recently, in-fiber linear polarizers based on 45°-TFGs have been reported with polarization extinction ratio as high as 35dB in none PM fibers [15-16]. By UV-inscribing a 45°-TFG in PM fiber along the fast- (or slow-) axis, an in-fiber polarizer with linear polarization output is achievable. Based on this, we have recently proposed and demonstrated all fiber Lyot filters [17]. In this paper, we present highly sensitive temperature and strain sensors based on all-fiber 45°-TFG based Lyot filter structures. The all-fiber Lyot filter was fabricated by splicing two 45°-TFGs UV-inscribed in PM fibers and a section of PM fiber cavity at 45° to its polarization axis. The sensing experiment results have shown that the Lyot filters have extremely high sensitivities to temperature and strain in comparison with FBGs.

2. STRUCTURE AND THEORY

The structure of an all-fiber Lyot filter is shown in Fig. 1. It employs a section of PM fiber as the birefringence material and two 45°-TFGs UV-inscribed in the same PM fiber along fast- (or slow-) axis as linear polarizers. The PM fiber cavity is sandwiched between the two 45°-TFGs with its polarization axis aligned at 45° to the fast- (or slow-) axis of the host PM fibers of 45°-TFGs.

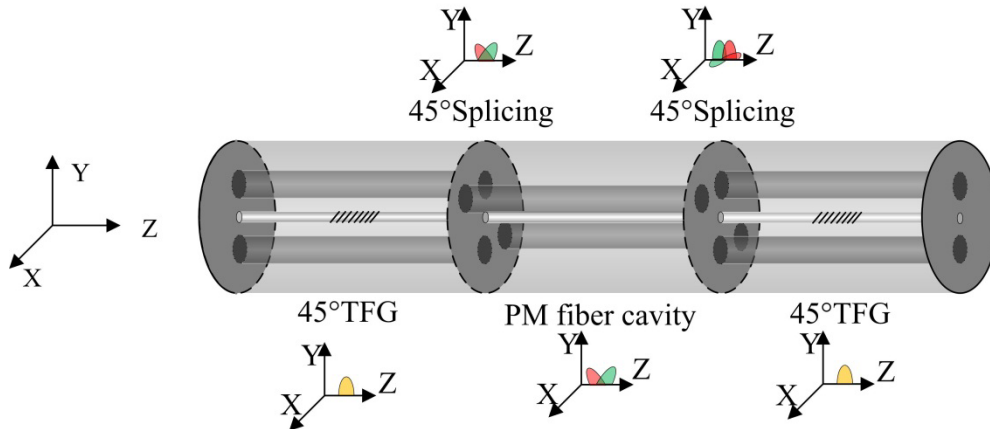


Fig. 1 The configuration of an all-fiber Lyot filter consisting of two 45°-TFGs segmented by a PM fiber cavity.

The working principle of the Lyot filter can be described as: the light transmitted through the first 45°-TFG will be linearly polarized, then enter the PM fiber cavity at 45° with respect to its fast- or slow-axis. The linear polarization light will be subsequently resolved into the fast- and slow-axis with equal amplitude, co-propagating in the PM fiber cavity. As the two beams propagating, a wavelength dependent phase difference $\Delta\phi$ will be induced due to the length and birefringence of the PM fiber cavity. Finally, when the two beams meet at the second 45°-TFG, they will be combined generating interference of linear polarization. The normalized transmittance of the light passed through the all-fiber Lyot filter is given by [17]:

$$T = \cos^2(\Delta\phi/2) = \cos^2\left(\frac{\pi L_{PM} \Delta n}{\lambda}\right) \quad (1)$$

Where, $\Delta\phi$ is the relative phase difference; L_{PM} is the length of PM fiber cavity; Δn is the birefringence of PM fiber and the λ is the working wavelength.

The maximum or minimum transmission of interference occurs when $\Delta\phi=2m\pi$ or $(2m+1)\pi$ ($m=0, 1, 2, 3\dots$). The wavelength of the max or min transmittance could be given by:

$$\lambda_{max}^m = \frac{L_{PM}\Delta n}{m} \quad \text{OR} \quad \lambda_{min}^m = \frac{2L_{PM}\Delta n}{2m+1} \quad (2)$$

By differentiating equation (2), the wavelength shift of m^{th} minimum transmission band of Lyot filter induced by temperature variation could be expressed as:

$$d\lambda_{min}^m = \frac{L_{heating}\lambda_{min}^m}{L_{PM}} \left(\frac{dL_{heating}}{L_{heating}dT} + \frac{d\Delta n}{\Delta n dT} \right) \Delta T \quad (3)$$

Where, $L_{heating}$ is the length of PM fiber cavity under heating, $dL_{heating}/(L_{heating}dT)$ is the thermal expansion coefficient (for silica fiber, it is $0.5 \times 10^{-6}/^\circ\text{C}$); and $d\Delta n/(\Delta n dT)$ is the thermal optical coefficient of birefringence of PM fiber (it is around $1 \times 10^{-3}/^\circ\text{C}$).

The expression of strain sensitivity of an all-fiber Lyot filter could be defined as:

$$d\lambda_{min}^m = \lambda_{min}^m \left(\frac{dL}{L_{PM}d\varepsilon} + \frac{d\Delta n}{\Delta n d\varepsilon} \right) \Delta\varepsilon \quad (4)$$

The $d\Delta n/(\Delta n d\varepsilon)$ is the elastic-optical coefficient of birefringence of PM fiber. It has been reported that the changing of birefringence of PM fiber with an axial strain is very small and nearly ignored. Because the axial strain cannot induce extra asymmetry to the fiber structure, the birefringence of PM fiber thus will not change, when the fiber is subjected to an axial strain[18]. So, the equation (4) could be simplified as:

$$d\lambda_{min}^m = \lambda_{min}^m \frac{dL}{L_{PM}d\varepsilon} \Delta\varepsilon = \lambda_{min}^m \frac{L_{strain}}{L_{PM}} \Delta\varepsilon \quad (5) \quad \text{Where,}$$

$d\varepsilon=dL/L_{strain}$; dL and L_{strain} are the increment and the PM fiber length under axial strain, respectively.

The temperature and strain effects of birefringence of PM fiber are two very critical parameters and a number of papers have reported the analysis for such effects [19-20]. In the work reported in this paper, we used an FBG UV-inscribed in PM fiber to estimate $d\Delta n/(\Delta n dT)$ and $d\Delta n/(\Delta n d\varepsilon)$. Their expressions could be given by:

$$\frac{d\Delta n}{\Delta n dT} = \frac{d\Delta\lambda_{PM}}{\Delta\lambda_{PM}dT} - \frac{d\Lambda_B}{\Lambda_B dT} \quad (6)$$

$$\frac{d\Delta n}{\Delta n d\varepsilon} = \frac{d\Delta\lambda_{PM}}{\Delta\lambda_{PM}d\varepsilon} - \frac{d\Lambda_B}{\Lambda_B d\varepsilon} \quad (7)$$

Where, $\Delta\lambda$ is the spacing between the two Bragg peaks with orthogonal polarization status.

3. FABRICATION AND PER RESPONSE OF 45°-TFGs

The two 45°-TFGs used in all-fiber Lyot filters were UV inscribed in PM fiber (purchased from Corning) using the scanning phase-mask technique and a 244nm UV source from a CW frequency doubled Ar⁺ laser (Coherent Sabre

Fred®). The PM fiber was hydrogen loaded at 150bar at 80°C for two days to induce photosensitivity. After UV-inscription, the 45°-TFGs were characterized for their polarization extinction ratio (PER) by the LUNA optics analysis system. The PER spectrum of the two 45°-TFGs were shown in Fig. 2. The measuring range is from 1525nm to 1605nm. Inset figure shows the polarization distribution of the 45°-TFGs (the detailed measuring method was introduced in ref. 13, 14). The near-perfect figure “8” shows the linear polarization property of the 45°-TFG in PM fiber.

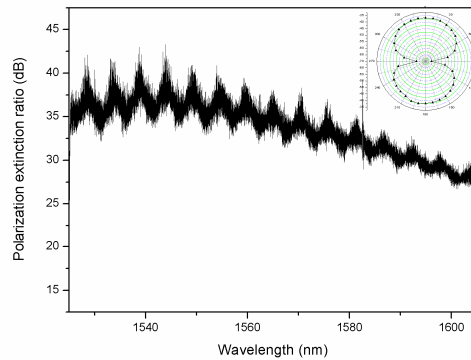
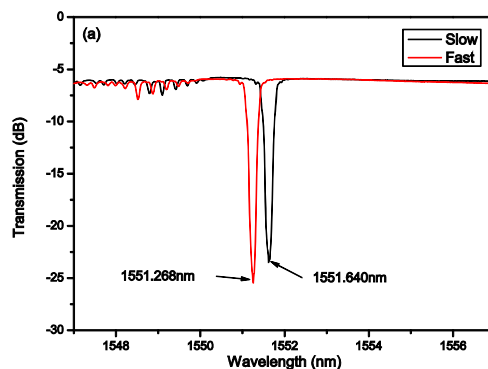


Fig. 2 The PER spectrum of the two 45°-TFG inscribed in PM fiber, showing a quite flat response over ~80nm range. Inset: the polarization distribution of the 45°-TFG in PM fiber.

4. SENSING EXPERIMENT AND RESULTS

4.1 The temperature and strain effects on birefringence of PM fiber

The temperature and strain effects on birefringence of PM fiber can be estimated by measuring the spacing between the fast- and slow-axis Bragg peaks of the FBG inscribed in PM fiber under heating and strain. Fig. 3 (a) shows the transmission spectra of the FBG inscribed in a PM fiber, showing two polarization Bragg peaks. Here, the spacing ($\Delta\lambda$) between the two polarization Bragg peaks is around 0.372 nm. With increasing temperature, the birefringence of the PM fiber, which can be measured by the spacing between the two polarization peaks, is reducing, but showing almost no change under the strain, as shown in Fig. 3 (b) and (c). The fiber birefringence changes with temperature at a rate of -4.5×10^{-4} nm/°C (see Fig. 3 (b)). The fact that the birefringence of the FBG is not changing with strain is because the fiber symmetry is not affected by axial strain, thus no extra birefringence induced.



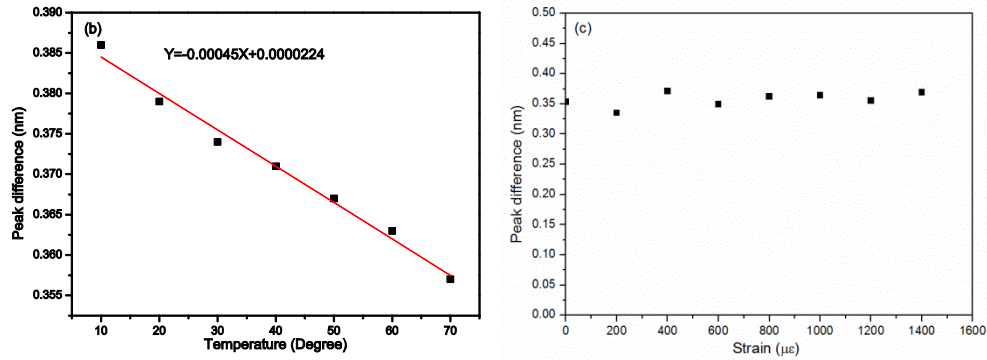


Fig. 3 (a) The transmission spectra of FBG inscribed in a PM fiber; the PM fiber birefringence (i.e. the spacing between the two polarization peaks) versus (b) temperature and (c) strain.

4.2 Temperature sensing

The temperature sensing experiment setup for all-fiber Lyot filter is shown in Fig. 4. A peltier with a temperature controller was used to heat a section of the Lyot filter cavity. Two 45°-TFG based Lyot filters with cavity lengths of 18cm and 40cm were subjected to the temperature sensing experiment. The middle section of the cavity about 6cm long was attached on the surface of the peltier (see Fig. 4). The cavity was heated from 10°C to 40°C with an increment of 5°C, precisely set by the temperature controller.

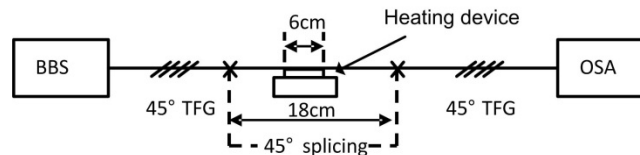
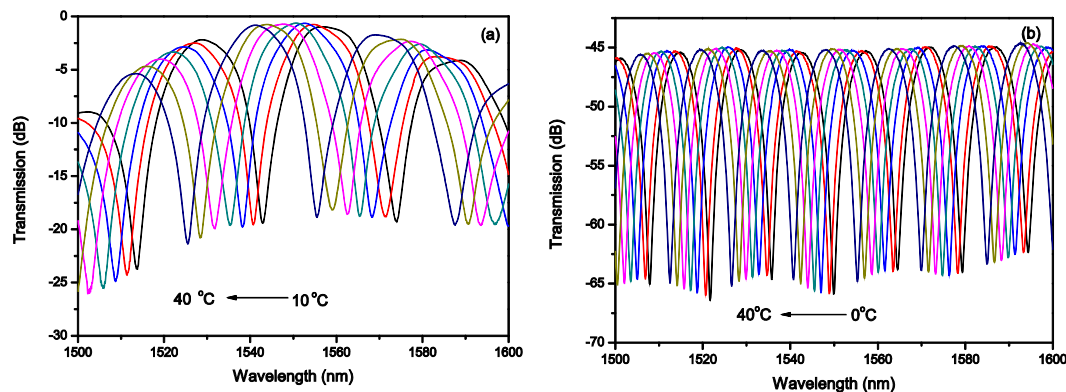


Fig. 4 Experiment setup for temperature sensing using the all-fiber Lyot filter.

When the part of cavity is heated up, due to thermal-expansion and thermal-optic effects on the fiber birefringence, the effective cavity of the filter will change, resulting in phase change between the two beams travelling along the fast- and slow-axis, thus inducing change to the transmission spectrum. Fig. 5 (a) and (b) show the spectral evolution of the 45°-TFG based all-fiber Lyot filters with cavity lengths of 18cm and 40cm, respectively.



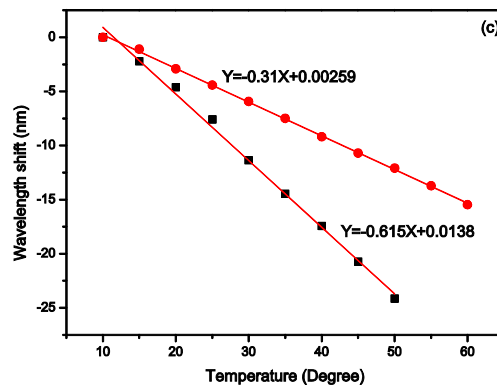


Fig. 5 The transmission spectra with increasing temperature from 10°C to 40°C for the two all-fiber Lyot filters with cavity lengths of (a) 18cm and (b) 40 cm; (c) the wavelength shift under the temperature tuning for (■) 18cm and (●) 40 cm long PM fiber cavity.

According to Equation (3), the temperature sensing sensitivity of an all-fiber Lyot filter is linearly proportional to the heating length of the PM fiber. For a 6 cm heating length, the sensitivities of 18cm- and 40cm-PM fiber cavity based all fiber Lyot filter are theoretically estimated around $-0.63\text{nm}/^\circ\text{C}$ and $-0.284\text{ nm}/^\circ\text{C}$, respectively. The measured temperature induced wavelength shift of the two filters are plotted in Fig. 5 (c) and from the plots, we can estimate the temperature sensitivities are around $-0.616\text{ nm}/^\circ\text{C}$ and $-0.31\text{ nm}/^\circ\text{C}$, which are in very good agreement with the theoretical results. It must be pointed out that 45°-TFG based Lyot filter has extremely high sensitivity in temperature. In comparison with the typical sensitivity of $10\text{pm}/^\circ\text{C}$ for standard FBGs, the demonstrated temperature sensitivities of the 45°-TFG based Lyot filters are several hundred times higher.

4.3.3 Strain sensing

The setup for strain sensing is shown in Fig. 6 (a). A section of the PM fiber cavity of the filter was clamped by two stages, and one of these stages could be controlled by a micrometer. In the strain sensing experiment, the filter with 18 cm long cavity was evaluated with stretching lengths of 18cm and 9cm. For the Lyot filter, the strain sensitivity is dependent on not just the stretching fiber length but also the monitoring wavelength. We have monitored the transmission peak around 1537nm under the strain change from 0 to $550\mu\epsilon$ and to $1100\mu\epsilon$ for the entire (18cm) and a half (9cm) of the cavity length under stretching. The strain induced spectral evolution is shown in Fig. 6 (b) and the strain responses are plotted in Fig. 6 (c). From Equation (5), we may calculate the strain sensitivities for the two designed all-fiber Lyot filters are $0.01537\text{nm}/\mu\epsilon$ and $0.00768\text{nm}/\mu\epsilon$, but the experiment results shown in Fig. 6(c) give the strain sensitivities of $0.02499\text{nm}/\mu\epsilon$ and $0.012\text{nm}/\mu\epsilon$ for 18cm and 9cm stretched lengths. The fact that measured strain sensitivity values are higher than that calculated could be due to some conditions associated with the experiment, which can be further investigated in future. The strain sensitivity is inversely proportional to the stretching fiber length and is also much higher than that of standard FBGs.

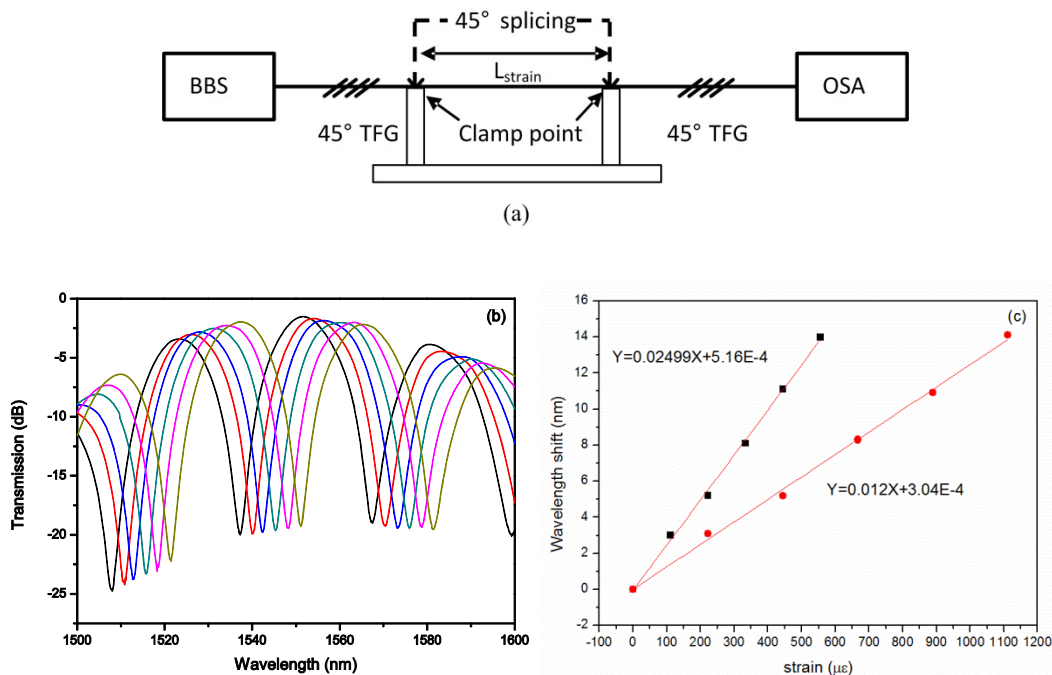


Fig. 6 (a) The setup for all-fiber Lyot filter strain experiment; (b) the transmission spectra of the Lyot filter with a 18cm long PM fiber cavity under axial strains; (c) the wavelength shift of 1537nm peak under strains from 0 to 550 $\mu\epsilon$ when 18cm cavity under stretch (■) and from 0 to 1100 $\mu\epsilon$ when 9cm cavity under stretch (●).

5. Conclusions

We have constructed all-fiber Lyot filters using two 45°-TFGs UV-inscribed in PM fiber as linear polarizers and segmented with a PM fiber cavity. The temperature and strain sensing property of such all-fiber Lyot filters have been theoretically analyzed and experimentally evaluated. The theoretical and experimental results for temperature response are in good agreement but with some discrepancy for strain. For temperature and strain sensing, the shorter cavity length gives higher sensitivity, as for such a filter the sensitivity is inversely proportional to the cavity length. As an example, we have demonstrated a temperature sensitivity of 0.616nm/C for the all-fiber Lyot filter designed with 18cm cavity length. This is remarkably high as it is almost 600 times higher than that of a standard FBG. More significantly, this may be utilized for a wavelength tuning filter of linear polarization output for a broad tuning range with simple and low-cost temperature tuning. These types of filters should find the use in optical fiber sensing and fiber laser applications.

6. Reference

- [1] H. J. Patrick, *et al.*, "Hybrid fiber Bragg grating/long period fiber grating sensor for strain/temperature discrimination," *Photonics Technology Letters, IEEE*, vol. 8, pp. 1223-1225, 1996.
- [2] Y. Yu, *et al.*, "Fiber Bragg grating sensor for simultaneous measurement of displacement and temperature," *Opt. Lett.*, vol. 25, pp. 1141-1143, 2000.

- [3] P. Kronenberg, *et al.*, "Relative humidity sensor with optical fiber Bragg gratings," *Opt. Lett.*, vol. 27, pp. 1385-1387, 2002.
- [4] R. Willsch, *et al.*, "Optical fiber grating sensor networks and their application in electric power facilities, aerospace and geotechnical engineering," in *Optical Fiber Sensors Conference Technical Digest, 2002. Ofs 2002, 15th*, 2002, pp. 49-54 vol.1.
- [5] G. M. a. J. M. W. William W. Morey, "Recent advances in fiber-grating sensors for utility industry applications " *Proc. SPIE*, vol. 90, p. 2594, 1996.
- [6] R. Maaskant, *et al.*, "Fiber-optic Bragg grating sensors for bridge monitoring," *Cement and Concrete Composites*, vol. 19, pp. 21-33, 1997.
- [7] X. Shu, *et al.*, "Dependence of temperature and strain coefficients on fiber grating type and its application to simultaneous temperature and strain measurement," *Opt. Lett.*, vol. 27, pp. 701-703, 2002.
- [8] J. Villatoro, *et al.*, "Photonic crystal fiber interferometer for chemical vapor detection with high sensitivity," *Opt. Express*, vol. 17, pp. 1447-1453, 2009.
- [9] B. Dong, *et al.*, "Temperature- and phase-independent lateral force sensor based on a core-offset multi-mode fiber interferometer," *Opt. Express*, vol. 16, pp. 19291-19296, 2008.
- [10] A. D. Kersey, *et al.*, "A SIMPLE FIBER FABRY-PEROT SENSOR," *Optics Communications*, vol. 45, pp. 71-74, 1983.
- [11] B. Lyot, "Optical apparatus with wide field using interference of polarized light,," *C.R. Acad. Sci. (Paris)*, vol. 197, p. 1593, 1933.
- [12] A. Gorman, *et al.*, "Generalization of the Lyot filter and its application to snapshot spectral imaging," *Opt. Express*, vol. 18, pp. 5602-5608, 2010.
- [13] H. Ming-Fang, *et al.*, "210-km bidirectional transmission system with a novel four-port interleaver to facilitate unidirectional amplification," *Photonics Technology Letters, IEEE*, vol. 18, pp. 172-174, 2006.
- [14] C. O'Riordan, *et al.*, "Lyot filter based multiwavelength fiber ring laser actively mode-locked at 10 GHz using an electroabsorption modulator," *Optics Communications*, vol. 281, pp. 3538-3541, 2008.
- [15] K. Zhou, *et al.*, "High extinction ratio in-fiber polarizers based on 45° tilted fiber Bragg gratings," *Opt. Lett.*, vol. 30, pp. 1285-1287, 2005.
- [16] Z. Yan, *et al.*, "UV-Inscription, Polarization-Dependant Loss Characteristics and Applications of 45° Tilted Fiber Gratings," *J. Lightwave Technol.*, vol. 29, pp. 2715-2724, 2011.
- [17] Z. Yan, *et al.*, "All-fiber polarization interference filters based on 45°-tilted fiber gratings," *Opt. Lett.*, vol. 37, pp. 353-355, 2012.
- [18] C. Guanghui, *et al.*, "Simultaneous strain and temperature measurements with fiber Bragg grating written in novel Hi-Bi optical fiber," *Photonics Technology Letters, IEEE*, vol. 16, pp. 221-223, 2004.
- [19] W. Honghai, *et al.*, "Effect of Temperature and Bending on PANDA Polarization-maintaining Fibers Fabricated by PCVD Method," in *Photonics Global@Singapore, 2008. IPGC 2008. IEEE*, 2008.
- [20] F. Zhang and J. W. Y. Lit, "Temperature and strain sensitivity measurements of high-birefringent polarization-maintaining fibers," *Appl. Opt.*, vol. 32, pp. 2213-2218, 1993.